Noninvasive EEG Correlates of Overground and Stair Walking

Justin A. Brantley, Trieu Phat Luu, Recep Ozdemir, Fangshi Zhu, Anna T. Winslow, Helen Huang, *Senior Member,* and Jose L. Contreras-Vidal*, Senior Member, IEEE*

***Abstract*—Automated walking intention detection remains a challenge in lower-limb neuroprosthetic systems. Here, we assess the feasibility of extracting motor intent from scalp electroencephalography (EEG). First, we evaluated the corticomuscular coherence between central EEG electrodes (C1, Cz, C2) and muscles of the shank and thigh during walking on level ground and stairs. Second, we trained decoders to predict the linear envelope of the surface electromyogram (EMG). We observed significant EEG-led corticomuscular coupling between electrodes and sEMG (tibialis anterior) in the high delta (3 -4 Hz) and low theta (4-5 Hz) frequency bands during level walking, indicating efferent signaling from the cortex to peripheral motor neurons. The coherence was increased between EEG and vastus lateralis and tibialis anterior in the delta band (< 2 Hz) during stair ascent, indicating a task specific modulation in corticomuscular coupling. However, EMG was the leading signal for biceps femoris and gastrocnemius coherence during stair ascent, possibly representing afferent feedback loops from periphery to the motor cortex. Decoder validation showed that EEG signals contained information about the sEMG patterns during over ground walking, however, the accuracy of the predicted sEMG patterns decreased during the stair condition. Overall, these initial findings support the feasibility of integrating sEMG and EEG into a hybrid decoder for volitional control of lower limb neuroprostheses.**

I. Introduction

Active assisted or assist-as-needed control strategies in rehabilitation robotics and neuroprotheses have been shown to enhance therapeutic outcomes [1]. In this control scheme, the powered wearable robots constantly estimate voluntary motor commands or motor intent from the users to control the device. Detection of human motor intent is achieved through human-machine physical interaction using motion and force sensors. However, this approach is not effective due to the time delay between the users' intention estimation and the robotic system's reaction. An alternative approach is non-physical interaction, which use muscle activities and brain activities to detect users' intent.

Myoelectric (EMG)-based assistance has proven to be effective for joint-oriented control of lower-limb exoskeletons and prosthetic devices during over ground walking [2-5]. However, there are some drawbacks to this approach, such as the interference of neighboring muscle signals on EMG recording, motion, and changing skin properties (e.g., sweat on skin), or limited residual muscle mass, such as after amputation.

Recent studies have shown that continuous lower limb kinematics can be decoded from noninvasive scalp EEG in both offline and real-time applications [6-8]. Similarly, the feasibility of detecting discrete users' intent from EEG signals has also been demonstrated [9, 10]. However, with the exception of [6], decoding of lower limb surface EMG patterns from cortical activity has not been demonstrated. Moreover, no studies have explored the feasibility of combined EEG and EMG control for continuous and discrete state detection during complex walking tasks.

Neurological signals provide a viable way to discern intent during feedback and feed-forward motor control tasks such lower limb movements during complex gait tasks. In this study, we seek to understand the time and frequency relationship between cortical and peripheral signaling during gait through simultaneous EEG and EMG recordings. We hypothesize that the EMG activations of lower limb muscles are preceded by low frequency modulations in the motor cortex during walking on various terrains. Additionally, we propose that low frequency EEG can be used to predict the EMG activation patterns of lower limb muscles during continuous walking, further demonstrating the feasibility of a hybrid EEG-EMG NMI architecture.

II. Methods

A. Experimental Setup

IRB approval was obtained from the University of North Carolina at Chapel Hill and the University of Houston. One thirty-one year old able-bodied male subject was enrolled in this feasibility study. EEG data were recorded wirelessly at 1000 Hz from 64-channels using active Ag/AgCl electrodes across the whole scalp (positioned according to a modified 10-20 international system) (BrainAmp DC, Brain Products, GmbH, Morrisville, NC). Channels FT9 and FT10 were then moved to the 10/20 locations for ground and reference to obtain information at the locations AFz and FCz, respectively. Channels TP9, PO9, PO10, and TP10, were removed from the cap and utilized for electrooculography (EOG) to measure eye-movement related artifacts during the experiments. Electrode impedance was maintained below 15 kΩ.

Twelve surface EMG electrodes (Motion Lab Systems, Baton Rouge, LA, USA) were mounted bilaterally on *rectus femoris (RF), vastus lateralis (VL), semitendinosus (SEM), biceps femoris (BF), medial gastrocnemius (GA),* and *tibialis anterior (TA)* muscles, and placed relative to anatomical landmarks [11]. The signals were referenced to the iliac crest

*This research is partly supported by NSF awards 1361549, 1406750 and IIS-1302339.

JB, PL, RO, FZ, and JLCV are with the Dept. of Electrical & Computer Engineering, University of Houston, TX 77004 USA. Phone: 713-743-0796; fax: 713-743-4444; [jabrantley, jlcontreras-vidal]@uh.edu.

AW and HH are with the NCSU/UNC Department of Biomedical Engineering, NC State University, Raleigh, NC, 27695; University of North Carolina at Chapel Hill, Chapel Hill, NC 27599

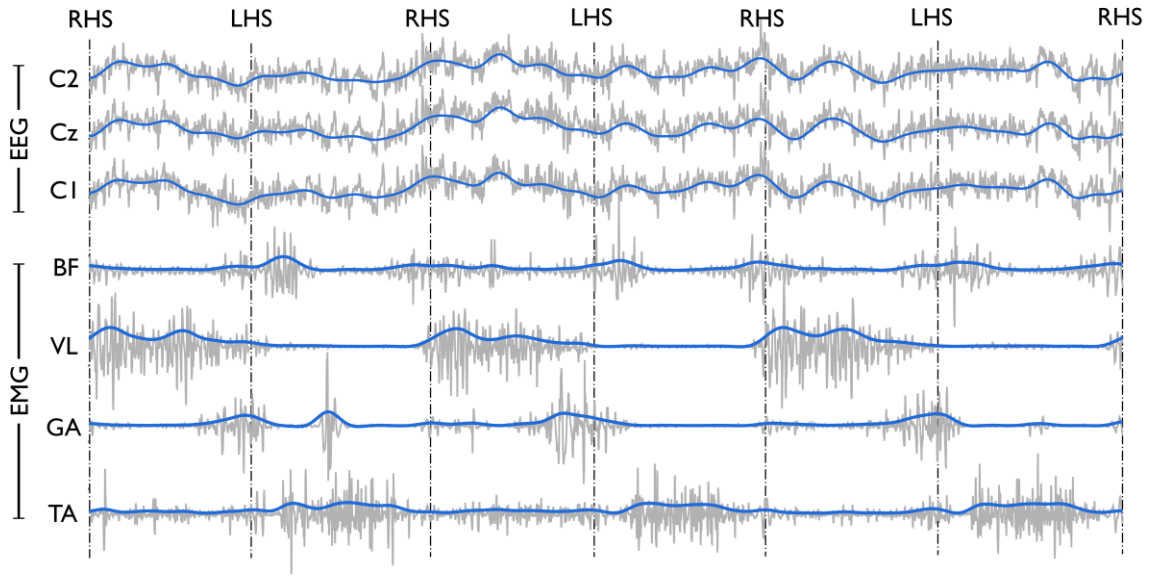

Figure 1. Filtered (blue) and raw (grey) EEG and EMG during stair ascent

and sampled at 1000 Hz. Heel strike (HS) and toe off (TO) gait events were captu red at 100 Hz using insole pressure sensors (Pedar-X, Novel Electronics Inc., GmbH, Germany). All data recordings were time synchronized and all trials were video recorded.

B. Experimental Procedure

The subject was asked to walk a straight section of level ground followed by (26ft) ascent up an 8-step staircase (13.4 cm step height). One trial consisted of four instances of level walking followed by stair ascent.

C. Signal Processing

The EEG signals were cleaned using Artifact Subspace Reconstruction (ASR) [12], [9] then band-pass filtered between 0.1 and 6 Hz using a 4th order zero-phase Butterworth filter. The EMG signals were high-pass filtered at 30 Hz, low-pass filtered at 300 Hz, then low pass filtered at 6 Hz to extract the linear envelope (all were 3rd order zero-phase Butterworth filters). The EEG and EMG were resampled to 100 Hz, which included an FIR low-pass filter to prevent aliasing. Figure 1 shows an example of the processed EEG and EMG during the stair ascent condition. The insole foot pressure sensors were used to segment the gait cycles into left HS, left TO, right HS, and right TO. The gait cycles were labeled by terrain and the time indices were utilized to segment the EEG and EMG data into time-locked epochs.

1) EEG-EMG wavelet coherence

The relationship in time-frequency space between EEG and EMG was estimated using wavelet coherence methods [13]. The Crosswavelet and Wavelet Coherence package (http://noc.ac.uk/using-science/crosswavelet-wavelet-coherence) was used to compute wavelet coherence (WTC) between selected EEG channels (C1, Cz, C2) in the motor cortex and EMG activation patterns from muscles of the right leg (VL, BF, TA and GA) that act as primary flexors and extensors of the ankle and knee joints during human locomotion. The Morlet wavelet was selected as the mother wavelet and default parameters were set as one octave for 10 scales [13]. The localized coherence significance was evaluated using a Monte Carlo analysis with 100 iterations.

The WTC was computed for the full trial prior to segmentation by gait cycle. The sections of level walking and stair walking were isolated from each trial and further segmented into gait cycle epochs. The ensemble average of coherence was computed to estimate corticomuscular coupling during the gait cycle. Each gait cycle epoch was determined from the insole foot pressure measurements and was as the time period from right heel strike to the following right heel strike.

2) Unscented Kalman Filter Decoding

The nonlinear relationship between cortical activity and muscle activations poses a significant challenge for traditional decoding schemes. Linear decoders such as Wiener and Kalman filters are commonly used for BMIs [14-16] but may not be sufficient for capturing the complex relationship between brain and muscle signaling during dynamic over ground walking. The unscented Kalman filter (UKF) was developed to improve performance in the context of nonlinear estimation, and has been shown to be effective for real-time BMI applications [7, 15]. Previous studies have outlined the details of the UKF extensively [7, 15].

The EEG signals and EMG envelope were segmented from each of the trials to isolate level ground and stair walking. The data from each neural source and walking condition were concatenated to construct a single matrix for each terrain. The EEG data from the past (50 – 60 ms), lags = 5, were used to predict the EMG envelope in each condition. To quantify the performance of the UKF, we computed the Pearson's correlation coefficient (r-value) across 10-fold cross validation. In the cross-validation procedure, the EEG and EMG envelope were divided equally into 10 segments. Nine segments of data were used to train the UKF and the remaining segment was used as testing data.

III. RESULTS

A. EEG and EMG wavelet coherence analysis

Figure 2 shows the time frequency evolution of wavelet coherence between the three EEG channels (C1, Cz, C2) and the four right leg muscles (VL, BF, TA and GA) during ground level walking and stair ascent gait cycles. In addition to time-frequency coherence, we can discern the time- phase direction (black angled arrows) and significance levels against Brownian noise (shown as black contour lines). Phase direction is shown by the orientation of arrows such that arrows pointing directly to the right represents perfectly in phase relationship while arrows pointing straight left indicates a completely out of phase relationship. A straight downward arrow indicates that EEG is leading EMG with a phase angle of 90° whereas a straight upward arrow shows

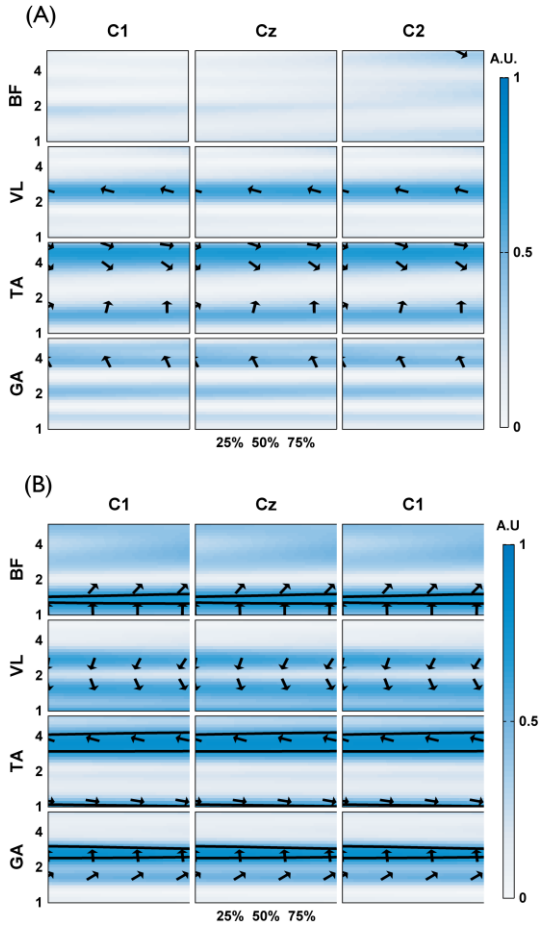

Figure 2. Pearson correlation (r-value) between predicted (UKF) and measured muscle activations on each condition.

the EMG is leading EEG with a phase angle of 90°.

Low (0.1) to moderate (0.5) coherences were observed between cortical activity and right leg muscle activation patterns during ground walking gait cycles (figure 2A). Phase angles indicated that EEG is leading the TA activation patterns at high delta (3 -4 Hz) and low theta oscillations (4-5 Hz). Coherences for VL, GA, and TA muscles, on the other hand, showed that EMG is the leading signal in the delta band (< 4 Hz, < 2 Hz for TA). During stair ascent gait cycles, significantly increased coherences were observed for all EEG channels and leg muscles (see figure 2B) indicating a task specific modulation in corticomuscular coupling. Specifically, EEG-led coherence was noticeably increased for VL in the delta band (0.1-4 Hz). Positive phase angles of the coherences indicate that slow cortical oscillations may also contain neural information regarding the general activation pattern of the lower limbs during human locomotion at different terrains. EEG-led coherence remained in the TA, but was mostly in very low delta, around 1 Hz. A significant increase in EMG-led coherence was observed in the BF (1-2 Hz), TA (~ 4 Hz), and GA (~3 Hz) muscles during stair ascent, possibly representing afferent feedback loops from periphery to the motor cortex.

B. UKF Decoding Results

Figure 3 shows the Pearson correlation coefficient (r-value) between the predicted (UKF) and measured EMG activation patterns during level walking and stair ascent. The best performance was found in decoding TA during over ground walking (r = 0.58) with the gastrocnemius having the second highest accuracy (r = 0.57). Overall, the average performance across 10-fold cross-validation for each muscle group was VL: 0.38 ± 0.07, TA: 0.49 ± 0.07, BF: 0.44 ± 0.09, and GA: 0.46 ± 0.06. During stair ascent, the UKF the GA had the highest accuracy (r = 0.42), followed closely by the BF (r = 0.38) and VL (r = 0.38). The average overall performance across 10-fold cross-validation during stair ascent was VL: 0.16 ± 0.08, TA: 0.05 ± 0.12; BF: 0.20 ± 0.11; GA: 0.19 ± 0.14). The results are noticeably lower during stair ascent, with the TA going from the highest accuracy during over ground walking to the lowest accuracy

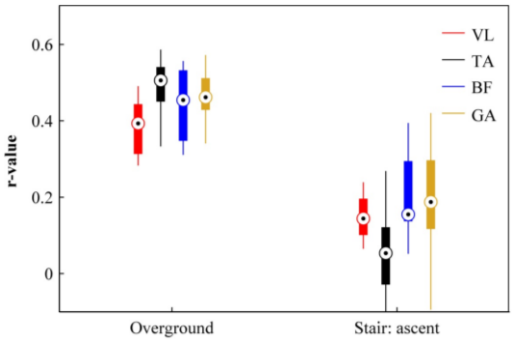

Figure 3. Pearson correlation (r-value) between predicted (UKF) and measured muscle activations on each condition.

during stair ascent.

Overall, these correlation values are comparable to previous studies on the decoding of lower limb kinematics (hip, knee, and ankle) during steady-state treadmill walking [7]. The results of the high TA decoding accuracies during over ground walking are corroborated by the coherence results, which revealed that the TA activations are led by EEG in the 4-6 Hz range. The noticeably lower decoding accuracies during stair ascent are reflected in the coherence analysis, which shows that EMG activations lead EEG the majority of the time. The exception is the VL, which is led by EEG by approximately 90°. The decoding results do not

appear to be affected by the leading EEG, which may be explained by the lack of statistical significance.

One possible explanation for the obtained correlation values during stair walking is difficulty in making predictions due to the non-linear dynamics of the experimental walking conditions. There are three notable challenges faced in this study. First, the walking speed was self-selected, thus the velocity was not constant, unlike walking on a treadmill at a single speed. Second, the terrain changes very rapidly and dramatically. The muscle activation profiles distinctly shift during stair walking versus level walking, and since the subject transitions to and from the conditions without stopping, the kinematics and muscle activations are likely also changing with time, especially at the transitions of each terrain. Lastly, the subject completed twenty trials for each condition, which may not be sufficient for accurate training of the UKF. More trials may be required to improve due to the variability within and between trials.

IV. Conclusions

In general, our coherence results extend previous studies by showing that, in addition to upper extremity tasks, which require fine motor control of hand muscles, corticomuscular coherence is also present during human locomotion. Our findings represent the involvement of the sensorimotor cortex in functional movements and lower limb muscle control for both muscle activation and afferent feedback signaling. We also showed task specific (level ground walking vs stair ascent) shifts in corticomuscular coupling from ankle flexors to knee flexor\extensors. Future NMI studies should develop decoding algorithms that consider task and muscle (TA vs GA) specific modulations in corticomuscular coupling. Low frequency EEG features showed high coherence with the EMG activation patterns and can be integrated to EMG based NMI algorithms to improve muscle activation pattern decoding and early detection of movement intentions and task transitions during locomotion.

Future work should consider two possibilities when predicting the EMG envelope from EEG. First, the timing of the information encoding the activation may be encoded at specific times prior to the movement. Second, more work needs to be completed to evaluate the roles of efferent vs afferent signaling in corticomuscular coupling, which may become more apparent as the other areas of the cortex are explored.

The complex nature of dynamic walking leads to the idea that ambulation is driven by a combination of feed-forward and feedback signaling, simultaneously combining internal models and sensory feedback [17, 18]. Thus, the ideal NMI would utilize signaling from both the central and peripheral nervous systems to incorporate both feedback and feed-forward information. A hybrid EEG-EMG NMI is a viable way to interpret movement intent through amplitude and frequency modulated central and peripheral nervous signaling.

References

[1] L. Marchal-Crespo and D. J. Reinkensmeyer, "Review of control strategies for robotic movement training after neurologic injury," *Journal of neuroengineering and rehabilitation,* vol. 6, p. 20, 2009.

[2] H. Huang, F. Zhang, L. J. Hargrove, Z. Dou, D. R. Rogers, and K. B. Englehart, "Continuous locomotion-mode identification for prosthetic legs based on neuromuscular-mechanical fusion," *IEEE Trans Biomed Eng,* vol. 58, pp. 2867-75, Oct 2011.

[3] H. Huang, F. Zhang, Y. L. Sun, and H. He, "Design of a robust EMG sensing interface for pattern classification," *J Neural Eng,* vol. 7, p. 056005, Oct 2010.

[4] M. R. Tucker, J. Olivier, A. Pagel, H. Bleuler, M. Bouri, O. Lambercy*, et al.*, "Control strategies for active lower extremity prosthetics and orthotics: a review," *J Neuroeng Rehabil,* vol. 12, p. 1, 2015.

[5] Y. Sankai, "HAL: Hybrid assistive limb based on cybernics," in *Robotics Research*, ed: Springer, 2010, pp. 25-34.

[6] Y. He, K. Nathan, A. Venkatakrishnan, R. Rovekamp, C. Beck, R. Ozdemir*, et al.*, "An integrated neuro-robotic interface for stroke rehabilitation using the NASA X1 powered lower limb exoskeleton," in *Engineering in Medicine and Biology Society (EMBC), 2014 36th Annual International Conference of the IEEE*, 2014, pp. 3985-3988.

[7] L. Trieu Phat, H. Yongtian, S. Brown, S. Nakagome, and J. L. Contreras-Vidal, "A closed-loop brain computer interface to a virtual reality avatar: Gait adaptation to visual kinematic perturbations," in *Virtual Rehabilitation Proceedings (ICVR), 2015 International Conference on*, 2015, pp. 30-37.

[8] A. Presacco, R. Goodman, L. Forrester, and J. L. Contreras-Vidal, "Neural decoding of treadmill walking from noninvasive electroencephalographic signals," *Journal of neurophysiology,* vol. 106, pp. 1875-1887, 2011.

[9] T. C. Bulea, S. Prasad, A. Kilicarslan, and J. L. Contreras-Vidal, "Sitting and Standing Intention Can be Decoded from Scalp EEG Recorded Prior to Movement Execution," *Frontiers in Neuroscience,* vol. 8, 2014.

[10] A. Kilicarslan, S. Prasad, R. G. Grossman, and J. L. Contreras-Vidal, "High accuracy decoding of user intentions using EEG to control a lower-body exoskeleton," *Conf Proc IEEE Eng Med Biol Soc,* vol. 2013, pp. 5606-9, 2013.

[11] A. Perotto and E. F. Delagi, *Anatomical guide for the electromyographer: the limbs and trunk*: Charles C Thomas Publisher, 2005.

[12] T. Mullen, C. Kothe, Y. M. Chi, A. Ojeda, T. Kerth, S. Makeig*, et al.*, "Real-time modeling and 3D visualization of source dynamics and connectivity using wearable EEG," *Conf Proc IEEE Eng Med Biol Soc,* vol. 2013, pp. 2184-7, 2013.

[13] A. Grinsted, J. C. Moore, and S. Jevrejeva, "Application of the cross wavelet transform and wavelet coherence to geophysical time series," *Nonlinear processes in geophysics,* vol. 11, pp. 561-566, 2004.

[14] H. A. Agashe, A. Y. Paek, Y. Zhang, and J. L. Contreras-Vidal, "Global cortical activity predicts shape of hand during grasping," *Frontiers in neuroscience,* vol. 9, 2015.

[15] Z. Li, J. E. O'Doherty, T. L. Hanson, M. A. Lebedev, C. S. Henriquez, and M. A. Nicolelis, "Unscented Kalman filter for brain-machine interfaces," *PLoS One,* vol. 4, p. e6243, 2009.

[16] A. Y. Paek, H. A. Agashe, and J. L. Contreras-Vidal, "Decoding repetitive finger movements with brain activity acquired via non-invasive electroencephalography," *Front. Neuroeng,* vol. 7, p. 10.3389, 2014.

[17] M. Desmurget and S. Grafton, "Forward modeling allows feedback control for fast reaching movements," *Trends in cognitive sciences,* vol. 4, pp. 423-431, 2000.

[18] R. Seidler, D. Noll, and G. Thiers, "Feedforward and feedback processes in motor control," *Neuroimage,* vol. 22, pp. 1775-1783, 2004.